Cell Reports, Volume *24*

Supplemental Information

Organoid Models of Human Liver Cancers

Derived from Tumor Needle Biopsies

Sandro Nuciforo, Isabel Fofana, Matthias S. Matter, Tanja Blumer, Diego Calabrese, Tujana Boldanova, Salvatore Piscuoglio, Stefan Wieland, Femke Ringnalda, Gerald Schwank, Luigi M. Terracciano, Charlotte K.Y. Ng, and Markus H. Heim

SUPPLEMENTAL INFORMATION

Figure S1

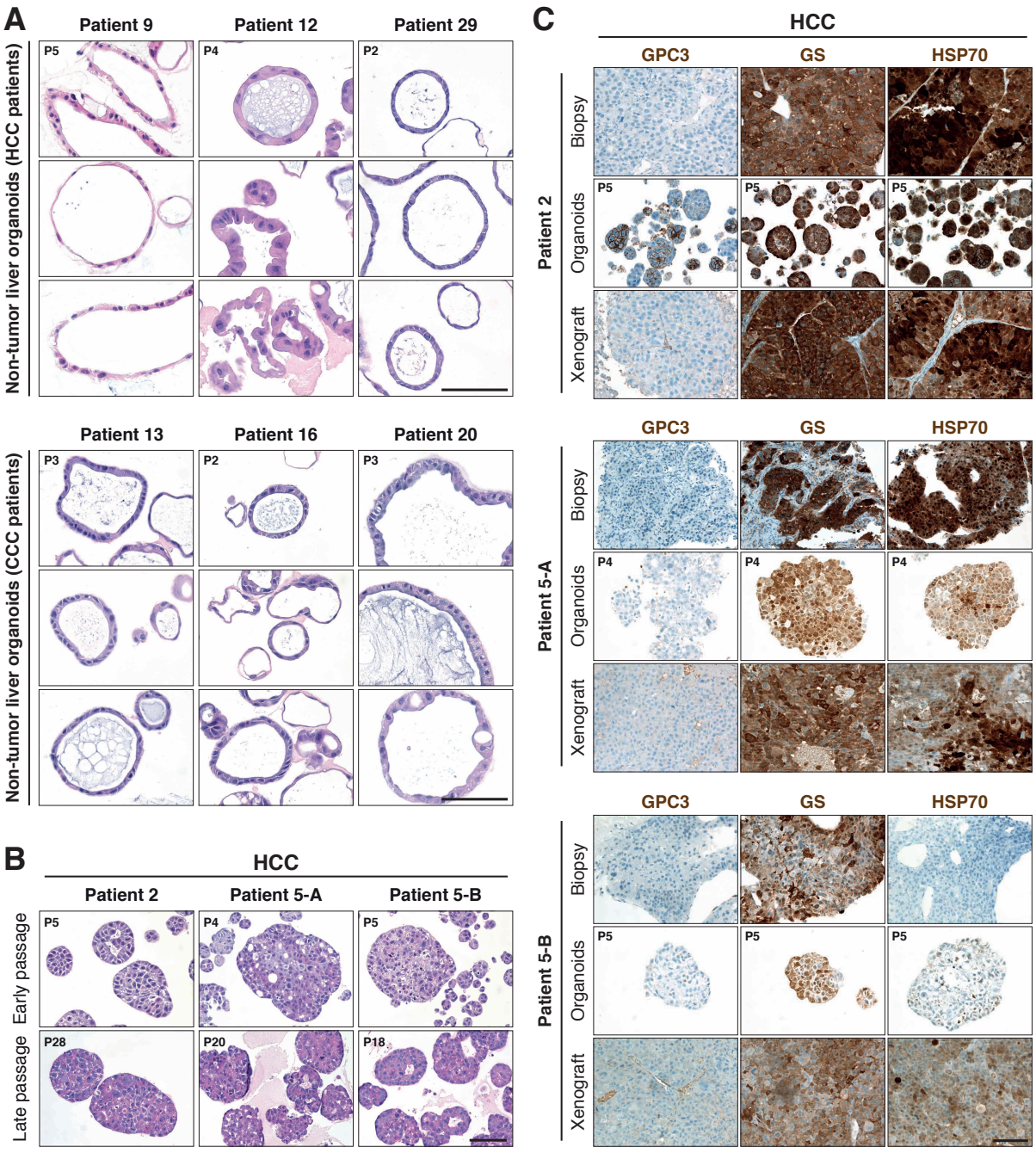

Figure S1. Histological Analysis of Tumor and Non-tumor Derived Organoids from HCC and CCC Patients. **Related to Figure 1, Figure 3 and Figure 4.** (**A**) Representative Hematoxylin and Eosin images of paired non-tumor liver organoids derived from HCC and CCC patients. Scale bars: 100 μm. (**B**) Representative Hematoxylin and Eosin images of HCC organoids at early and late passage (range P4-P28), showing no morphological differences after long-term culture. For Patient 2, HCC organoid culture time between early and late passage corresponds to 52 weeks, for Patient 5-A 29 weeks and Patient 5-B 26 weeks. Scale bar: 100 μm. (**C**) Histological sections of three representative HCC biopsies, their derivative organoids and organoid-derived xenografts stained for Glypican 3 (GCP3), Glutamine Synthetase (GS) and Heat Shock Protein 70 (HSP70) by immunohistochemistry. Organoids were imaged at the indicated passage numbers. Scale bar: 100 μm.

Figure S2

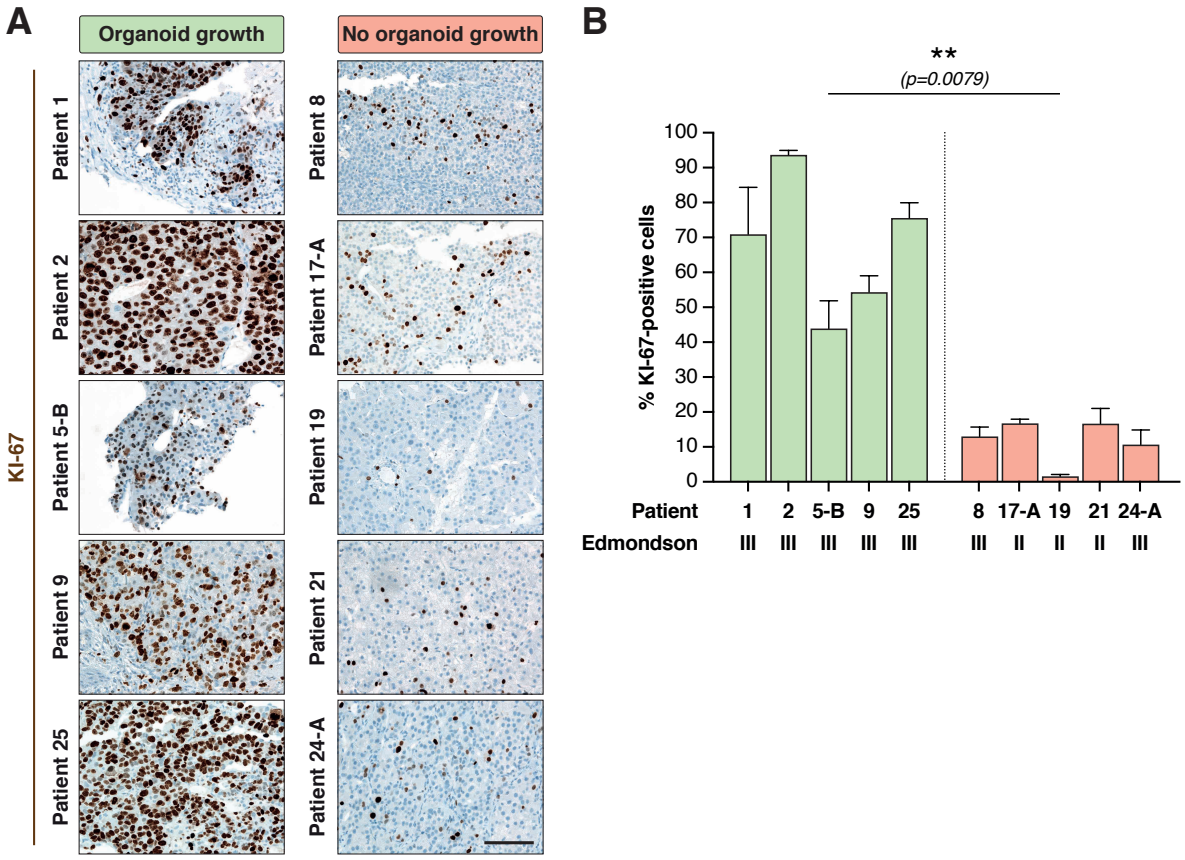

Figure S2. KI-67 Analysis on HCC Tumor Biopsies Used for Organoid Generation. Related to Figure 2. (**A**) Representative tissue sections of ten randomly chosen HCC biopsies stained for the proliferation marker KI-67 by immunohistochemistry. Tumors that did not result in organoid growth have only few KI-67-positive nuclei. Scale bar: 100 µm. (**B**) Quantification of KI-67-positive nuclei for the ten HCC biopsies (p=0.0079, two-tailed t-test). Shown is the mean ± SEM of at least three images for each tissue section and patient. Approximately 1'000 cells were counted per patient.

Figure S3

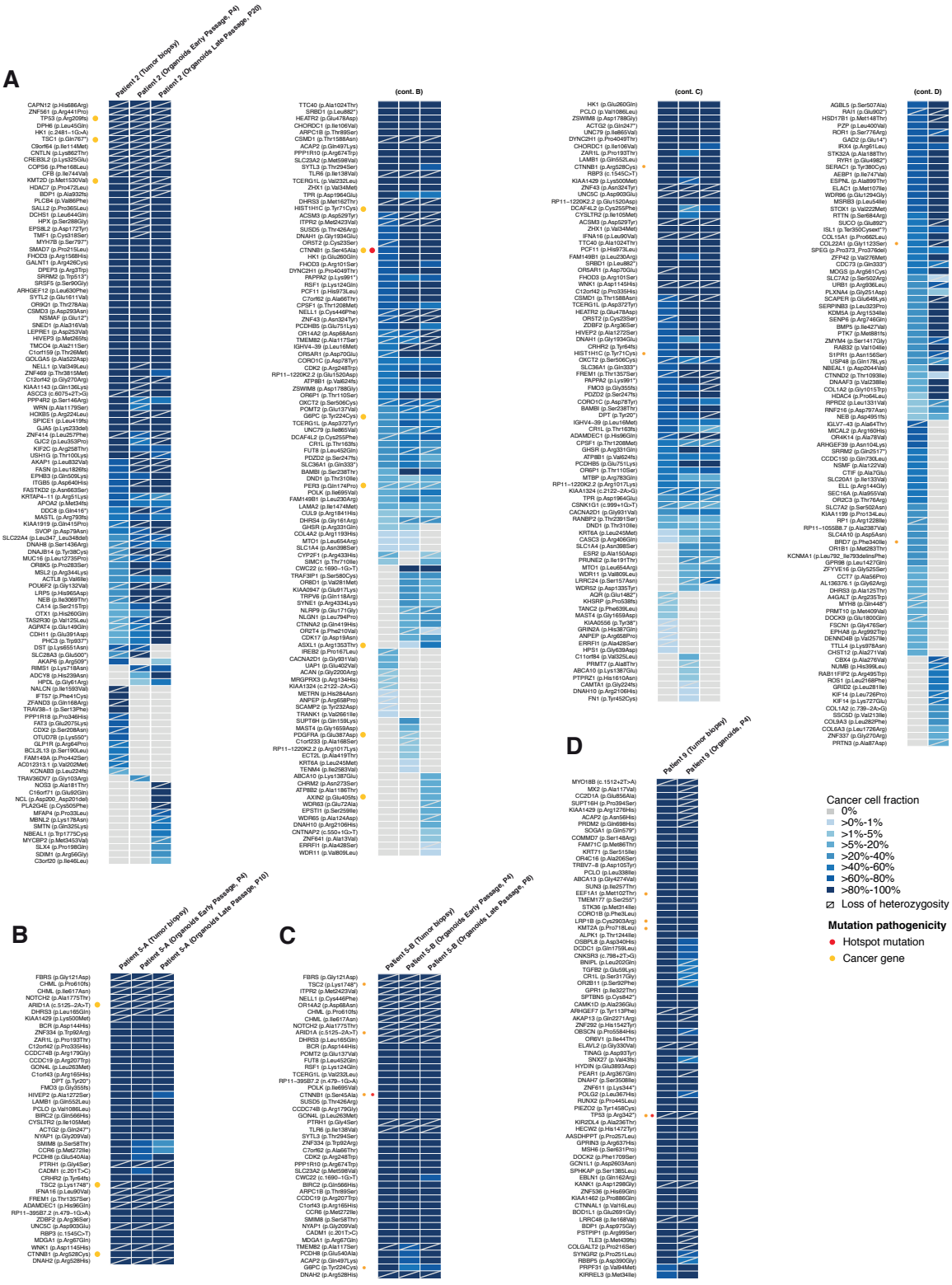
A
Patient 2 (Tumor biopsy)
Patient 2 (Organoids Early Passage, P4)
Patient 2 (Organoids Late Passage, P20)
(cont. B)
(cont. C)
(cont. D)
B
Patient 5-A (Tumor biopsy)
Patient 5-A (Organoids Early Passage, P4)
Patient 5-A (Organoids Late Passage, P10)
C
Patient 5-B (Tumor biopsy)
Patient 5-B (Organoids Early Passage, P4)
Patient 5-B (Organoids Late Passage, P8)
D
Patient 9 (Tumor biopsy)
Patient 9 (Organoids, P4)
Cancer cell fraction
0%
>0%-1%
>1%-5%
>5%-20%
>20%-40%
>40%-60%
>60%-80%
>80%-100%
Loss of heterozygosity
Mutation pathogenicity
Hotspot mutation
Cancer gene

Figure S3. Repertoire of Somatic Mutations in Tumor Biopsies and Derivative Organoids of Patients 2, 5-A, 5-B and 9. Related to Figure 5. Heatmaps indicate the cancer cell fraction of somatic non-synonymous autosomal mutations as determined by ABSOLUTE (Carter et al., 2012) (blue, see color key) or their absence (grey) in each sequenced HCC tumor biopsy/ HCC organoids (**A**-**D**). Mutations affecting cancer genes (Fujimoto et al., 2016; Kandoth et al., 2013; Lawrence et al., 2014) or hotspot residues (Chang et al., 2016; Gao et al., 2017) are indicated by yellow and red dots, respectively.

Figure S4

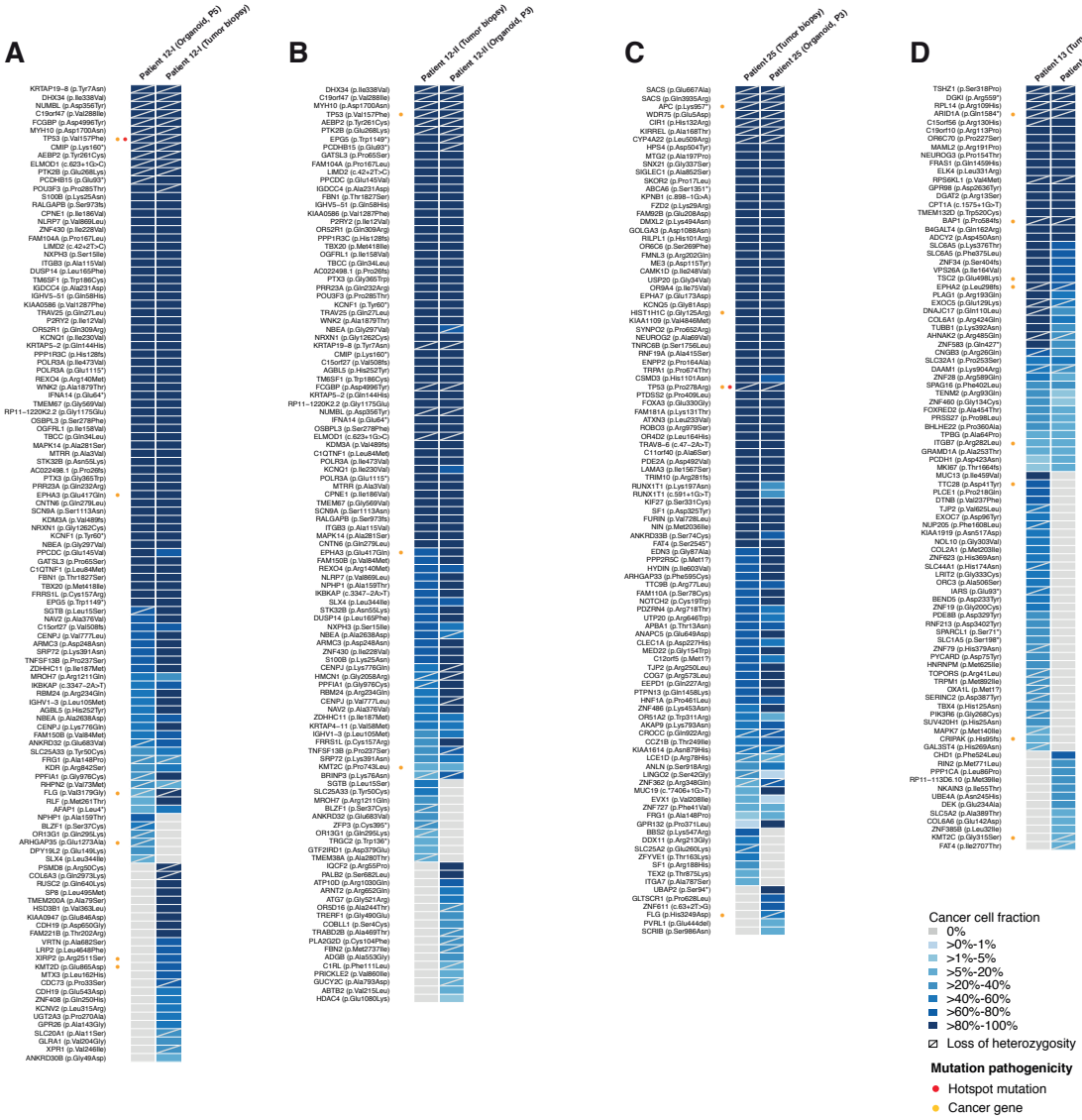
A
Patient 12-I (Organoid, P5)
Patient 12-I (Tumor biopsy)
B
Patient 12-II (Tumor biopsy)
Patient 12-II (Organoid, P5)
C
Patient 25 (Tumor biopsy)
Patient 25 (Organoid, P3)
D
Patient 13 (Tumor biopsy)
Patient 13 (Organoid, P1)
Cancer cell fraction
0%
>0%-1%
>1%-5%
>5%-20%
>20%-40%
>40%-60%
>60%-80%
>80%-100%
Loss of heterozygosity
Mutation pathogenicity
Hotspot mutation
Cancer gene

Figure S4. Repertoire of Somatic Mutations in Tumor Biopsies and Derivative Organoids in Patients 12-I, 12-II, 25 and 13. Related to Figure 5. Heatmaps indicate the cancer cell fraction of somatic non-synonymous autosomal mutations as determined by ABSOLUTE (Carter et al., 2012) (blue, see color key) or their absence (grey) in each sequenced HCC tumor biopsy/ HCC organoids (**A**-**D**). Mutations affecting cancer genes (Fujimoto et al., 2016; Kandoth et al., 2013; Lawrence et al., 2014) or hotspot residues (Chang et al., 2016; Gao et al., 2017) are indicated by yellow and red dots, respectively.

Figure S5

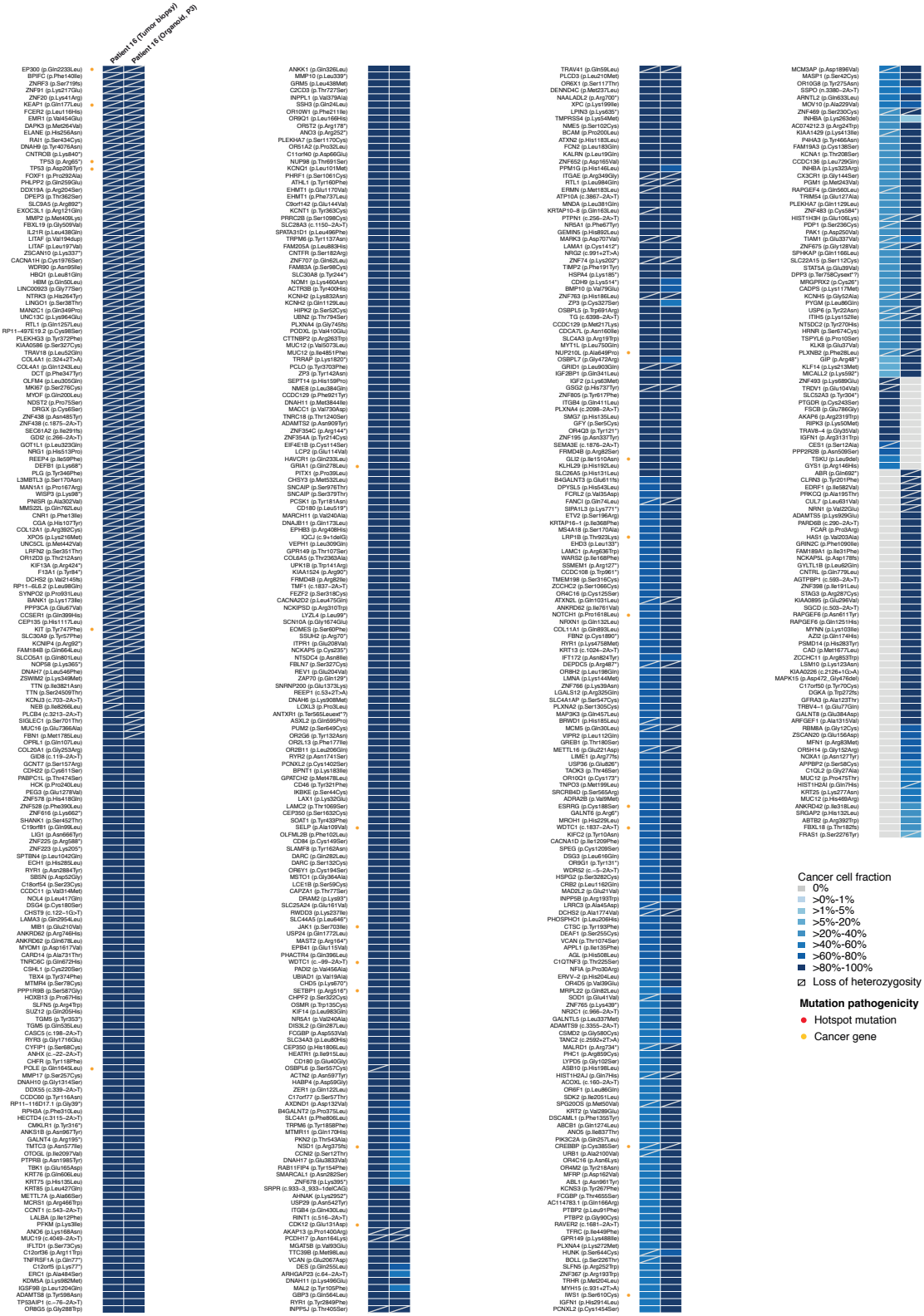
Patient 16 (Tumor biopsy)
Patient 16 (Organoid, P3)
Cancer cell fraction
0%
>0%-1%
>1%-5%
>5%-20%
>20%-40%
>40%-60%
>60%-80%
>80%-100%
Loss of heterozygosity
Mutation pathogenicity
Hotspot mutation
Cancer gene

Figure S5. Repertoire of Somatic Mutations in Tumor Biopsies and Derivative Organoids in Patient 16. Related to Figure 5. Heatmaps indicate the cancer cell fraction of somatic non-synonymous autosomal mutations as determined by ABSOLUTE (Carter et al., 2012) (blue, see color key) or their absence (grey) in each sequenced HCC tumor biopsy/ HCC organoids. Mutations affecting cancer genes (Fujimoto et al., 2016; Kandoth et al., 2013; Lawrence et al., 2014) or hotspot residues (Chang et al., 2016; Gao et al., 2017) are indicated by yellow and red dots, respectively.

Figure S6

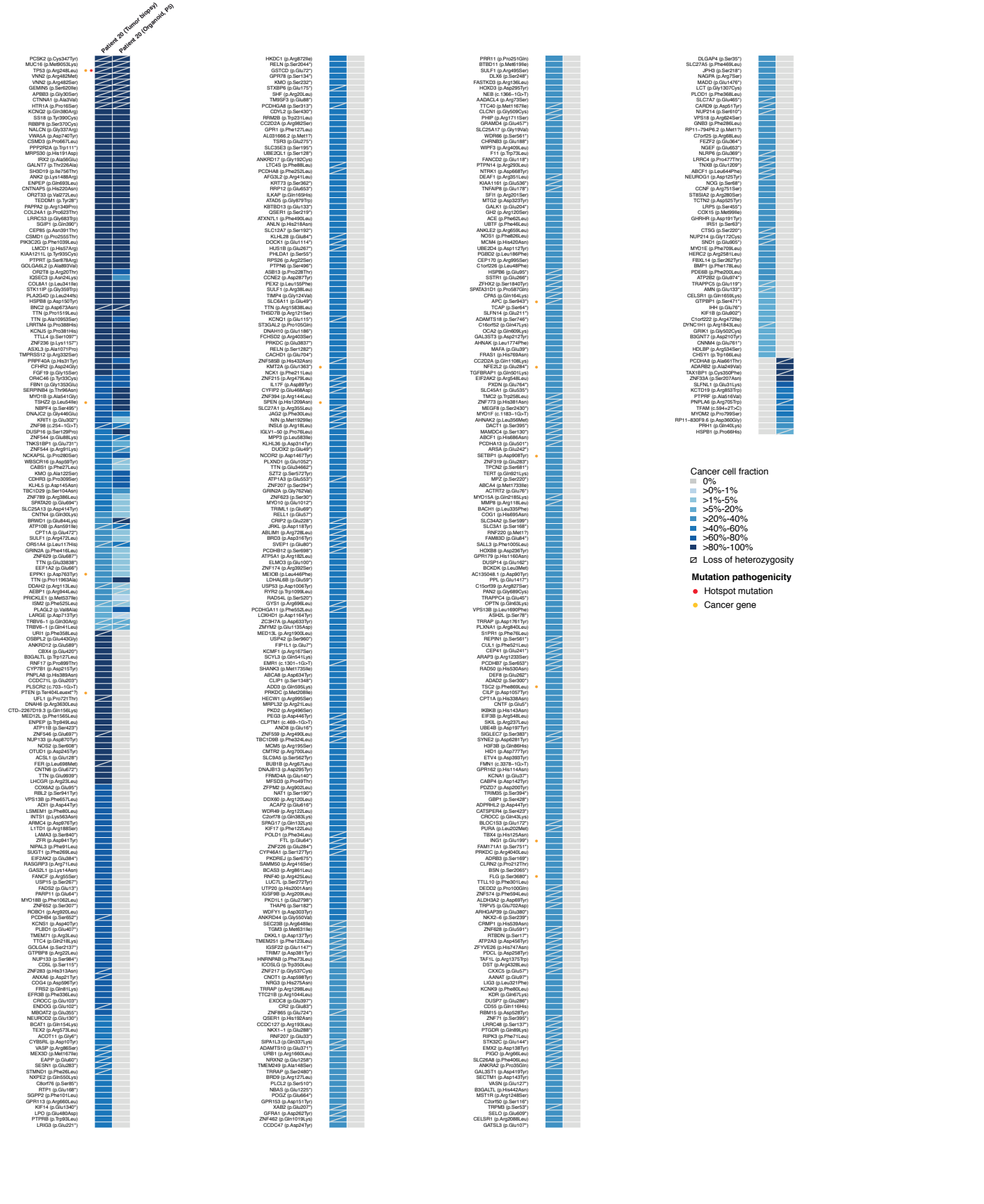
Patient 20 (Tumor biopsy)
Patient 20 (Organoid, P5)
Cancer cell fraction
0%
>0%-1%
>1%-5%
>5%-20%
>20%-40%
>40%-60%
>60%-80%
>80%-100%
Loss of heterozygosity
Mutation pathogenicity
Hotspot mutation
Cancer gene

Figure S6. Repertoire of Somatic Mutations in Tumor Biopsies and Derivative Organoids in Patient 20. Related to Figure 5. Heatmaps indicate the cancer cell fraction of somatic non-synonymous autosomal mutations as determined by ABSOLUTE (Carter et al., 2012) (blue, see color key) or their absence (grey) in each sequenced HCC tumor biopsy/ HCC organoids. Mutations affecting cancer genes (Fujimoto et al., 2016; Kandoth et al., 2013; Lawrence et al., 2014) or hotspot residues (Chang et al., 2016; Gao et al., 2017) are indicated by yellow and red dots, respectively.

Figure S7

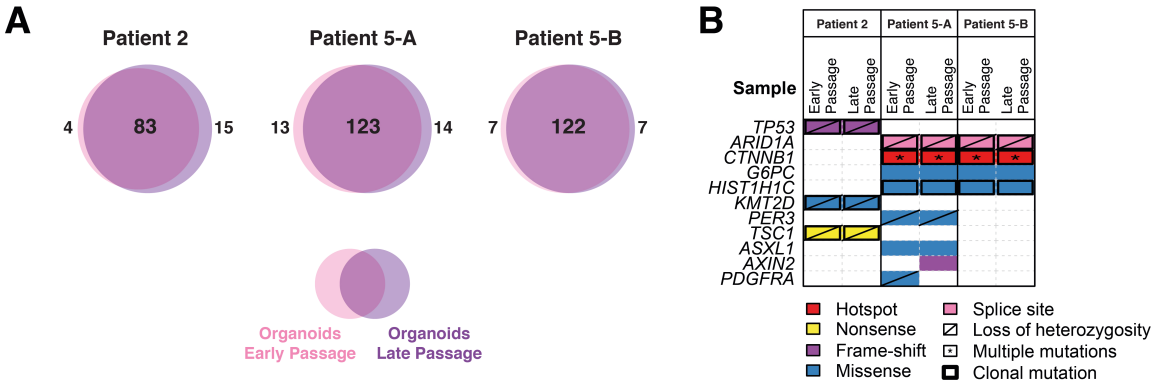
A
Patient 2
Patient 5-A
Patient 5-B
4
83
15
13
123
14
7
122
7
Organoids
Early Passage
Organoids
Late Passage
B
Patient 2
Patient 5-A
Patient 5-B
Sample
Early Passage
Late Passage
TP53
ARID1A
CTNNB1
G6PC
HIST1H1C
KMT2D
PER3
TSC1
ASXL1
AXIN2
PDGFRA
Hotspot
Nonsense
Frame-shift
Missense
Splice site
Loss of heterozygosity
Multiple mutations
Clonal mutation

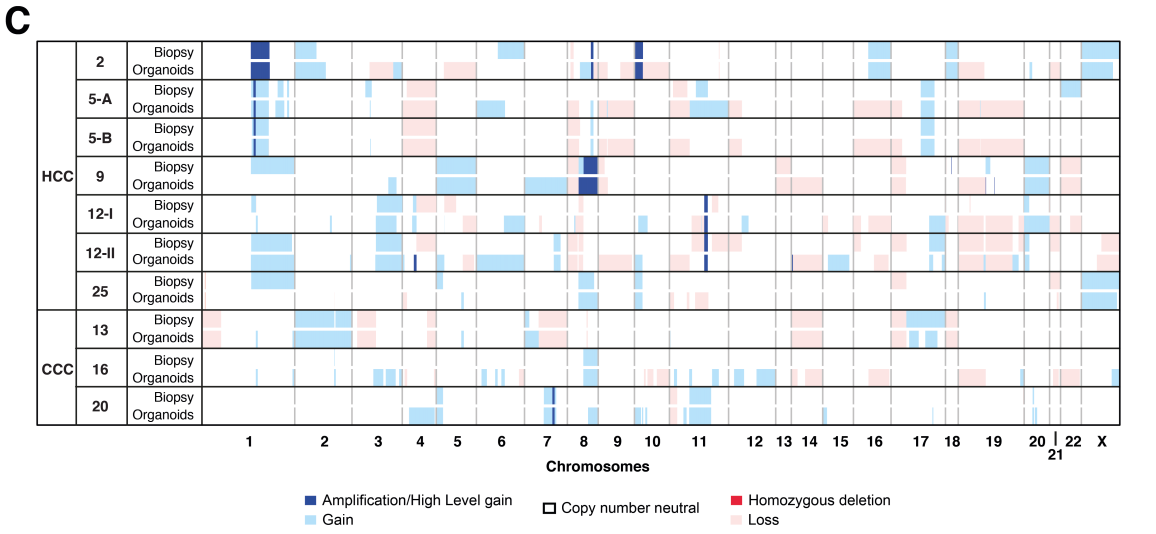
C
HCC
CCC
2
5-A
5-B
9
12-I
12-II
25
13
16
20
Biopsy
Organoids
1 2 3 4 5 6 7 8 9 10 11 12 13 14 15 16 17 18 19 20 21 22 X
Chromosomes
Amplification/High Level gain
Gain
Copy number neutral
Homozygous deletion
Loss

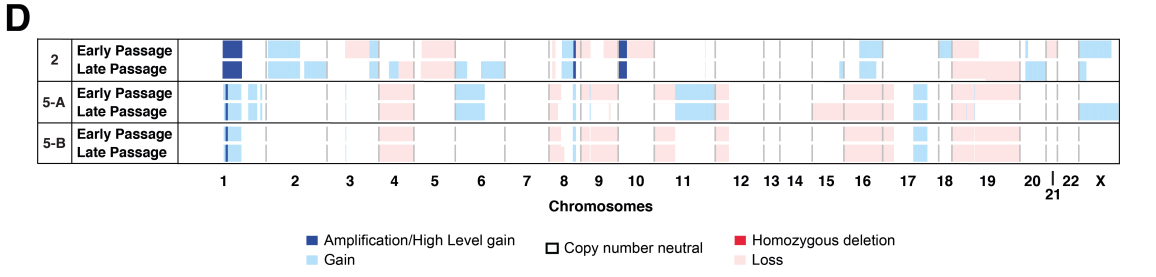
D
2
5-A
5-B
Early Passage
Late Passage
1 2 3 4 5 6 7 8 9 10 11 12 13 14 15 16 17 18 19 20 21 22 X
Chromosomes
Amplification/High Level gain
Gain
Copy number neutral
Homozygous deletion
Loss

Figure S7. Analysis of Long-term Genetic Stability in HCC and CCC Organoids. Related to Figure 5. (**A**) Venn diagrams illustrate the number of somatic non-synonymous mutations present in three representative HCC organoid lines at early and late passage. For whole exome sequencing analysis of the HCC organoids derived from Patient 2, culture time between early and late passage was 32 weeks, corresponding to 16 passages. For the HCC organoid lines 5-A and 5-B culture time was 8 weeks corresponding to 6 and 4 passages, respectively. (**B**) Repertoire of somatic non-synonymous mutations affecting cancer genes (Fujimoto et al., 2016; Kandoth et al., 2013; Lawrence et al., 2014) at early and late passage. The effects of the mutations are color-coded according to the legend, with hotspots (Chang et al., 2016; Gao et al., 2017) colored in red. The presence of multiple non-synonymous mutations in the same gene is represented by an asterisk. The presence of loss of heterozygosity of the wild-type allele of a mutated gene is represented by a diagonal bar, and mutations found to be clonal by ABSOLUTE (Carter et al., 2012) are indicated by a black box. (**C**) Heatmap of copy number alterations in HCC biopsies and derivative organoids (Patients 2, 5-A, 5-B, 9, 12-I, 12-II and 25) and CCC biopsies and derivative organoids (Patients 13, 16 and 20). Samples are presented in rows and chromosomal positions on the x-axis (columns). Dark blue: amplification, light blue: copy number gain; white: neutral; light red: copy number loss; dark red: homozygous deletion. (**D**) Heatmap illustrating the copy number alterations between early and late passage organoids.

Figure S8

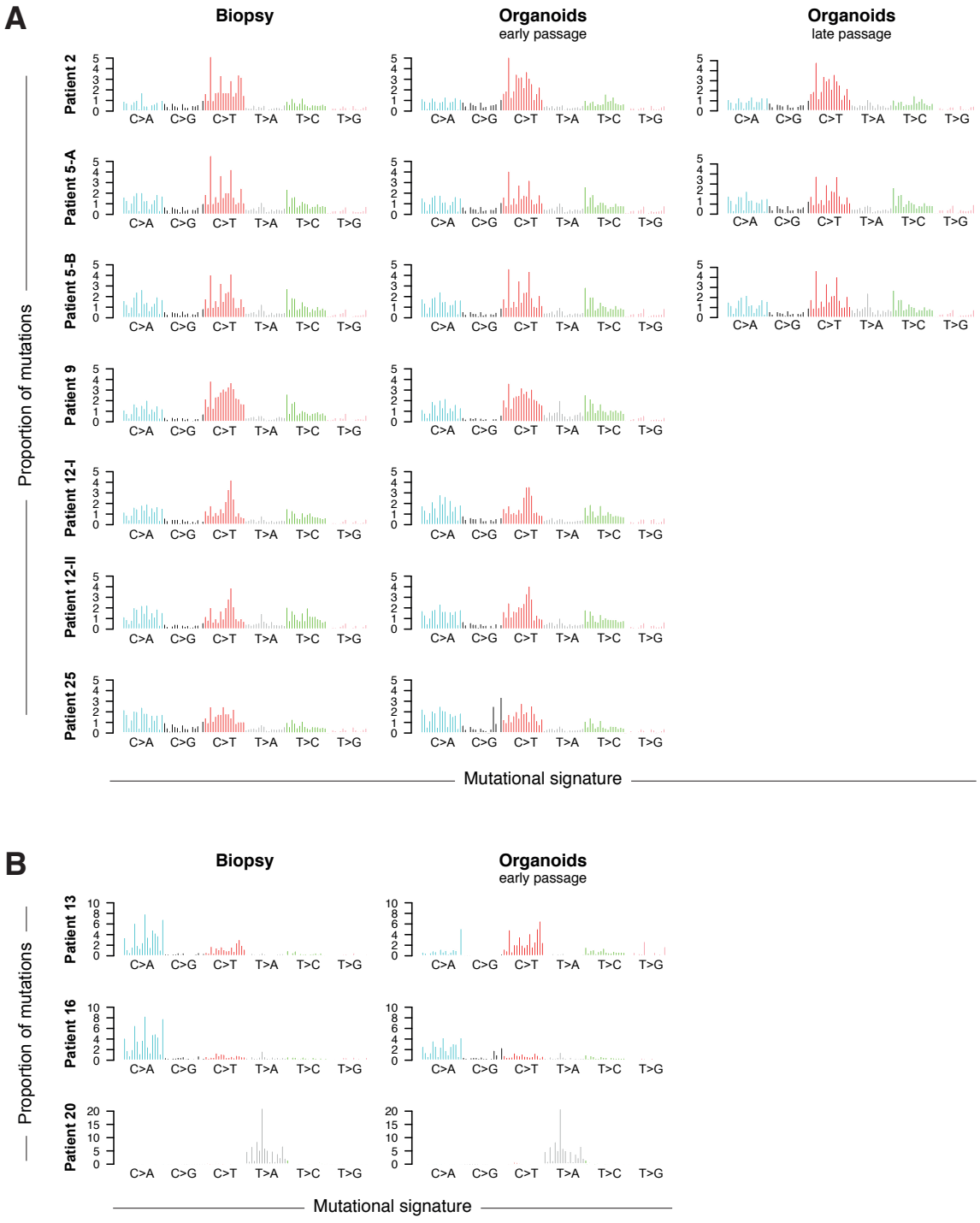
A
Biopsy
Organoids
early passage
Organoids
late passage
Patient 2
Patient 5-A
Patient 5-B
Patient 9
Patient 12-I
Patient 12-II
Patient 25
C>A C>G C>T T>A T>C T>G
Proportion of mutations
Mutational signature
B
Biopsy
Organoids
early passage
Patient 13
Patient 16
Patient 20
C>A C>G C>T T>A T>C T>G
Proportion of mutations
Mutational signature

Figure S8. Mutational Signatures in Tumor Biopsies and Derivative Organoids. Related to Figure 5. (**A**) Barplots illustrate the mutational signatures of the HCC biopsies and the corresponding organoids at early and late passage (late passage only for Patients 2, 5-A and 5-B). In each panel, the colored barplot illustrates each mutational signature according to the 96 substitution classification (Alexandrov et al., 2013) defined by the substitution classes (C>A, C>G, C>T, T>A, T>C and T>G bins) and the 5' and 3' sequence context, normalized using the observed trinucleotide frequency in the human exome to that in the human genome. The bars are ordered first by mutation class (C>A/G>T, C>G/G>C, C>T/G>A, T>A/A>T, T>C/A>G, T>G/A>C), then by the 5' flanking base (A, C, G, T) and then by the 3' flanking base (A, C, G, T). (**B**) Mutational signature for CCC biopsies and corresponding organoids.